Key Amino Acid Residues in the Regulation of Soluble Methane Monooxygenase Catalysis by Component B†

Brian J. Brazeau and John D. Lipscomb*

Department of Biochemistry, Molecular Biology, and Biophysics, and the Center for Metals in Biocatalysis, University of Minnesota, Minneapolis, Minnesota 55455

Received December 30, 2002; Revised Manuscript Received March 19, 2003

ABSTRACT: The regulatory component MMOB of soluble methane monooxygenase (sMMO) has been hypothesized to control access of substrates into the active site of the hydroxylase component (MMOH) through formation of a size specific channel or region of increased structural flexibility tuned to methane and O_2. Accordingly, a decrease in the size of four MMOB residues (N107G/S109A/S110A/T111A, the Quad mutant) was shown to accelerate the reaction of substrates larger than methane with the reactive MMOH intermediate **Q** [Wallar, B. J., and Lipscomb, J. D. (2001) *Biochemistry 40*, 2220−2233]. Here, this hypothesis is tested by construction of single and double mutations involving the residues of the Quad mutant. It is shown that mutations of residues that extend into the core structure of MMOB alter many aspects of the MMOH catalyzed reaction but do not mimic the effects of the Quad mutant. In contrast, the MMOB residues that are thought to form part of the interface in the MMOH−MMOB complex increase active site accessibility as observed for the Quad mutant. In particular, the mutant T111A mimics most of the effects of the Quad mutant; thus, Thr111 is proposed to most directly control access. Unexpectedly, mutation of Thr111 to the larger Tyr greatly increases the rate constant for the reaction of larger substrates such as ethane, furan, and nitrobenzene with **Q** while decreasing the rate constant for the reaction with methane. Other steps in the cycle are dramatically slowed, the regiospecificity for nitrobenzene oxidation is altered, and 10-fold more T111Y than wild-type MMOB is required to maximize the rate of turnover. Thus, T111Y appears to make a more extensive change in local interface structure that allows hydrocarbons at least as large as ethane to bind and react with **Q** similarly. As a result, the bond cleavage rates for methane, ethane, and their deuterated analogues are shown for the first time to correlate with bond strength in accord with a mechanism in which C−H bond cleavage occurs during reaction of substrates with **Q**.

The soluble form of methane monooxygenase (sMMO)[1] (*1*−*4*) isolated from methanotrophic bacteria catalyzes the oxygen and NADH coupled conversion of methane to methanol with the following stoichiometry:

$$NAD(P)H + H^+ + CH_4 + O_2 \rightarrow NAD(P)^+ + CH_3OH + H_2O$$

Our past studies have shown that both the oxygen activation and the methane oxidation reactions are catalyzed by the hydroxylase component of the sMMO (MMOH) utilizing an oxygen-bridged binuclear iron cluster at the active site (*5*). X-ray crystallographic studies show that both the iron cluster and the active site pocket of MMOH are buried within the protein, and there is no obvious access channel to admit substrates (*6*, *7*). The sMMO system also includes a reductase component (MMOR) containing FAD and a [2Fe−2S] cluster that serves to supply the two electrons required for catalysis (*5*, *8*) and an effector protein (MMOB) devoid of metals or cofactors that regulates the reaction (*5*, *9*, *10*).

Transient kinetic studies have shown that the binuclear cluster of MMOH passes through several intermediates during its catalytic cycle as shown in Scheme 1 (*11*−*14*). Briefly, the resting Fe(III)Fe(III) form of the cluster ($\mathbf{H^{ox}}$) is first reduced to the diferrous state ($\mathbf{H^{r}}$) that can react with O_2. This reaction occurs through an intermediate **O** in which the oxygen is apparently bound to the enzyme but not to the cluster. In the next two steps, oxygen binds to the cluster to form intermediate **P***, and then with the input of a proton, **P*** is converted to the bridging hydroperoxo intermediate **P** that exhibits a weak absorbance at 700 nm (*13*−*15*). Addition of a second proton (*14*) allows formation of intermediate **Q**, which has been shown to be a unique bis-μ-oxo binuclear Fe(IV) compound capable of reacting directly with hydrocarbons (*11*, *12*, *15*−*17*). **Q** exhibits a relatively intense chromophore at 430 nm, allowing it to be readily observed in the background of the other colorless or weakly colored intermediates. Although mechanistically controversial (*18*−*24*), the following step involves cleavage of the substrate C−H bond and insertion of an atom of oxygen to form the

† This work was supported by NIH Grant GM40466 (to J.D.L.). B.J.B. was supported in part by part by NIH Training Grant GM08277.

* To whom correspondence should be addressed. Telephone: (612) 625-6454. Fax: (612) 624-5121. E-mail: lipsc001@tc.umn.edu.

[1] Abbreviations: D, ^{2}H; KIE, kinetic isotope effect; sMMO, soluble methane monooxygenase; MMOH, sMMO hydroxylase component; MMOB, sMMO component B; MMOR, sMMO reductase; Quad mutant, MMOB mutant N107G/S109A/S110A/T111A; WT-MMOB, wild-type MMOB; MOPS, 3-[*N*-morpholino]propane-sulfonic acid; $\mathbf{H^{ox}}$, oxidized MMOH; $\mathbf{H^{r}}$, reduced MMOH; **O**, **P***, **P**, **Q**, **T**, compounds O, P*, P, Q, and T from the MMOH catalytic cycle.

10.1021/bi027429i CCC: $25.00
Published on Web 04/19/2003

Scheme 1: SMMO Catalytic Cycle[a]

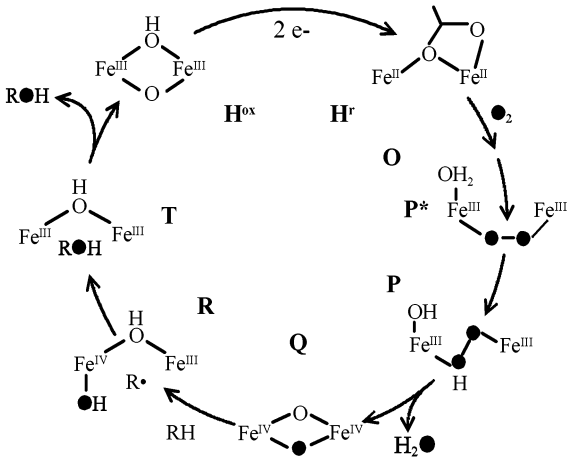

[a] The reaction is initiated by the reduction of the resting, diferric state of the enzyme with two electrons. In a multiple-turnover reaction with all three protein components present, NADH is the electron donor. In a single-turnover reaction the enzyme is reduced chemically, and the only other protein component required for rapid reaction is MMOB. The single letter nomenclature for each intermediate in the catalytic cycle is in the interior of the cycle adjacent to the appropriate schematic of the diiron center. The fate of labeled oxygen (filled O) is hypothetical although it is clear that one oxygen from O_2 is found in the product.

terminal product complex **T**. Release of product from **T** completes the cycle.

MMOB plays a critical role in regulating the rates of interconversion of several of the intermediates of the catalytic cycle. This was initially recognized by the fact that the bright yellow intermediate **Q** was not observed to accumulate if MMOB was omitted from the single-turnover reaction (*11*). This was later shown to be due to the fact that the initial reaction of oxygen with the cluster to form intermediates **P*** and **P** is 1000-fold slower in the absence of MMOB (*10*). It has been shown that this oxygen gating effect is a result of the formation of a specific complex between the α subunit of the $(\alpha\beta\gamma)_2$ MMOH and MMOB (*25*). The complex formation causes dramatic changes in the spectroscopic and electronic properties of MMOH as well as the regiospecificity of its reactions with complex substrates (*25*−*30*).

Recently, we have solved the solution structure of MMOB isolated from *Methylosinus trichosporium* OB3b (*31*) and identified many residues that might interact with MMOH using NMR approaches (*32*). Several of the potential interaction sites were then modified using site-directed mutagenesis (*33*). It was shown that specific classes of MMOB mutants could be defined that affect the rates of individual steps throughout the MMOH reaction cycle. One particularly interesting mutant involved changing four grouped MMOB residues (N107G/S109A/S110A/T111A) and was thus termed the Quad mutant. This mutation resulted in an acceleration of the reaction of **Q** with large substrates and also an acceleration of the release of large products from **T**. We hypothesized that MMOB may regulate the reaction of MMOH with substrates by facilitating the entry of substrates and release of products on the basis of their size. This effectively converts MMOH into a molecular sieve for methane and O_2, perhaps accounting for the remarkable fact that sMMO can selectively oxidize methane in a background of hydrocarbons with weaker C−H bonds. We postulated that in the Quad mutant, small hydrophobic residues replace larger hydrophilic residues, thereby adjusting the hole size of the sieve to accommodate larger molecules.

Like many other oxygenase enzymes, sMMO can catalyze the oxidation of a wide range of substrates. However, the only physiologically relevant substrate is methane. Accordingly, the reaction of methane with **Q** is unique in many ways, most remarkably, the fact that the reaction exhibits a ^{2}H-KIE of ∼50 (*17*), whereas all other substrates exhibit no observable isotope effect (*15*, *17*). Recently, we have shown that the reaction of **Q** with all substrates occurs in two steps, first forming an intermediate substrate complex (**QS**) (*15*). Kinetic studies suggest that the rate-limiting step of this process for all substrates except methane is the formation of **QS** (*15*, *34*). Since this means that the bond-breaking step is only rate limiting for methane, only the reaction with this substrate shows an isotope effect. Interestingly, an isotope effect is induced for the reaction of **Q** with ethane by the substitution of the Quad mutant for wild-type MMOB (WT-MMOB) in the reaction (*34*). We suggested that this is due to the ability of the Quad mutant to facilitate larger substrate binding and therefore shift the rate-limiting step from binding to C−H bond breaking in the case of ethane.

In the current paper, we probe the roles of the individual residues modified in the Quad mutant. It is shown that mutation of specific residues in this region of the MMOB surface cause profoundly different effects on catalysis at the MMOH reactive center. The results support the molecular sieve hypothesis, but they also serve to emphasize the exquisite effects of protein structure on catalysis for an enzyme that must generate and control one of the most powerful oxidizing reagents found in a biological system.

EXPERIMENTAL PROCEDURES

Reagents. All reagents were the highest grade available and purchased from either Sigma (St. Louis, MO) or Aldrich Chemicals (Milwaukee, WI).

Bacterial Growth and Protein Purification. MMOH and MMOR were purified from *M. trichosporium* OB3b as previously reported (*5*, *35*). The growth and purification of WT-MMOB from the recombinant system using *Escherichia coli* BL21(DE3) as the host was performed as previously reported (*31*, *33*), and the same procedures were used for each of the mutants used in this work. The optical properties of the mutants were found to be the same as observed for wild-type MMOB except for the T111Y mutant, which exhibited an increase in the extinction coefficient at 280 nm from 20.8 to 22.3 mM^{-1} cm^{-1}. This small increase in the extinction coefficient is in accord with that expected from the addition of a single tyrosine residue (ϵ_{280} = 1.4 mM^{-1} cm^{-1}). The increased extinction coefficient was consistent with the results of three independent methods of protein quantitation: (i) UV absorbance at 280 nm, (ii) the method of Bradford (*36*), and (iii) SDS−PAGE band intensity after staining.

Site-Directed Mutagenesis. The construction of the pB-WJ400 plasmid containing the WT-MMOB gene has been previously reported (*31*). All mutations made to the MMOB gene in this plasmid were performed using the QuikChange system from Stratagene (La Jolla, CA) according to the instructions from the manufacturer. Each mutation in the MMOB gene was confirmed by sequencing at the University

Table 1: Oligonucleotides Used to Induce Mutations in Plasmid pBWJ400 Containing the Wild-Type MMOB Gene

MMOB isoform	oligonucleotide sequence
DBL1	5′ CGACCTTCTCATCAACGTGGCGAGCGCGGTCGGCCGCGCC 3′ 3′ GCTGGAAGAGTAGTTGCACCGCTCGCGCCAGCCGGCGCGG 5′
DBL2	5′ CCTTCTCATCGCGGTGTCGGCGACGGTCGGCCGC 3′ 3′ GGAAGAGTAGCGCCACAGCCGCTGCCAGCCGGCG 5′
S109A	5′ CCTTCTCATCAACGTGGCGAGCACGGTCGGCCGCGCC 3′ 3′ GGAAGAGTAGTTGCACCGCTCGTGCCAGCCGGCGCGG 5′
T111A	5′ CATCAACGTGTCGAGCGCGGTCGGCCGCGCCTAC 3′ 3′ G TAGTTGCACAGCTCGCGCCAGCCGGCGCGGATG 5′
T111Y	5′ CATCAACGTGTCGAGCTATGTCGGCCGCGCCTAC 3′ 3′ GTAGTTGCACAGCTCGATACAGCCGGCGCGGATG 5′

of Minnesota Microchemical Facility. The oligonucleotides used to introduce the mutations to the MMOB gene are listed Table 1.

Transient Kinetic Experiments. The transient kinetic experiments were performed using an Applied Photophysics SX.18MV stopped-flow spectrophotometer (Surrey, UK). All transient kinetic experiments were done under single-turnover conditions as reported previously (*11*, *15*). For experiments monitoring the formation and decay of intermediates **P** and **Q**, the buffer was 50 mM MOPS, pH 7 or 7.6 as noted. Pseudo-first-order conditions were established with both oxygen and substrate in large excess over enzyme. Each experiment contained either 23 or 42 μM MMOH (active sites), as noted. In most experiments, the MMOB:MMOH (active sites) stoichiometry was 1:1, except in the case of the T111Y variant that was present in 10:1 excess because of a decreased affinity during turnover for MMOH (see Results). In all experiments monitoring the evolution of *p*-nitrophenol ($\epsilon_{404} = 15$ mM^{-1} cm^{-1} at pH 7.6), 1.6 mM nitrobenzene was used in 50 mM MOPS, pH 7.6 at 25 °C. The concentration of nitrobenzene in each experiment was made from an appropriate dilution of a saturated (16 mM) solution of nitrobenzene (Merck Index). The procedure for the double mix stopped-flow experiments using T111Y was previously described for a study using wild-type MMOB (*15*). The delay time for the second mix was chosen to be the time of maximal **Q** formation as determined from the time course monitored at 430 nm in the absence of substrates at 25 °C in 50 mM MOPS, pH 7 (see Figure 9A).

The analyses of the single-turnover time courses at 430 nm monitoring the formation and decay of **Q** and at 700 nm monitoring the formation and decay of **P** were performed using the program KFIT developed by N. C. Millar of Kings College (London, England). The reciprocal relaxation times were associated with the appropriate reaction step as described elsewhere (*11*, *15*).

The time course for nitrobenzene single turnover monitored at 404 nm has at least five species that contribute to the observed time course, making nonlinear regression fitting procedures using summed exponential equations less accurate. Thus, it was determined that the best way to extract rate constants from the data was by using a combination of nonlinear regression fitting and simulations using the numerical integration program KSIM also developed by N. C. Millar. The fitting procedure has been described elsewhere (*33*). The following mechanism was used to simulate the data:

$$\mathbf{H^r} \xrightarrow{k_1} \mathbf{O} \xrightarrow{k_2} \mathbf{P} \xrightarrow{k_3} \mathbf{Q} \xrightarrow{k_4} \mathbf{T} \xrightarrow{k_5} \mathbf{T1} \xrightarrow{k_6} \mathbf{H^{ox}} + p\text{-nitrophenol}$$

Relative extinction coefficients were determined for each species based upon experimentally determined values from SVD fitting procedures to nitrobenzene single-turnover experiments monitored using a diode array detector (*11*). Experimental parameters were identical to those described above for single-turnover experiments using the single wavelength detector. The rate constants used in the simulations were based on experimental values from data that have been previously published in most cases (*11*, *15*). In cases where the rate constants were not known, manual iterations were performed, and the rate constants were varied systematically to achieve a best fit to the data.

Steady-State Kinetic Experiments. All steady-state experiments were performed using an Applied Photophysics SX.18MV stopped-flow spectrophotometer. The reaction mixture contained 1 μM MMOH (active sites), 1 μM MMOB (or 10 μM T111Y), 1 μM MMOR, 100 μM NADH, and ambient concentration of O_2 (~250 μM). Each steady-state experiment was performed using 50 mM MOPS at 25 °C and pH 7.6. The same conditions were used in NADH turnover experiments whether in the presence of MMOR alone, or with MMOR and MMOB both present. In the absence of substrate, or when the substrates furan or methane were used, the reaction was followed by monitoring the consumption of NADH at 340 nm ($\epsilon_{340} = 6.23$ mM^{-1} cm^{-1}). When nitrobenzene was used as the substrate, the reaction was followed by monitoring the formation of the product *p*-nitrophenol at 404 nm.

The steady-state data were analyzed by linear regression of the linear portion of the reaction time course using the program KFIT. Saturated conditions were used when methane or furan was the substrate, and turnover numbers were calculated by dividing the slope obtained from linear regression fitting procedures by the appropriate extinction coefficient and the concentration of MMOH active sites. In nitrobenzene titration experiments, initial velocities were calculated by dividing the slope obtained from the fit to the data by the extinction coefficient for *p*-nitrophenol and the concentration of MMOH active sites.

Simulation of Single-Turnover Time Course at 430 nm with the T111Y and DBL1 Mutants. The simulation of the reaction time course of T111Y was completed using the program KSIM. The simulation was designed such that the rate constants for the formation and decay of intermediate **Q** and oxidized MMOH were drawn from experimental data recorded at 25 °C and were in agreement with previous results from our laboratory (*11*, *14*, *15*, *17*). The rate of **Q** formation in the simulation was determined from a nonlinear regression fit to the time course at 430 nm with the T111Y

variant. In the absence of substrates, there are no intermediates known to occur between **Q** and oxidized MMOH; thus, it was assumed that **Q** decays directly to the oxidized, diferric form of MMOH. Because intermediates **O**, **P***, and **P** all form within the dead time of the stopped-flow instrument at 25 °C, the rate constants used for the formation of each of these intermediates could not be experimentally determined. Thus, for the formation of **O**, **P***, and **P** rate constants of 1000, 500, and 250 s^{-1}, respectively, estimated by extrapolation of Arrhenius plots using data collected at lower temperatures were used. The simulation of the reaction time course when DBL1 was used was performed using a similar procedure. Three different features of the simulated time courses for the 700 and 430 nm data were compared with the actual data: (i) the t_{max}, (ii) the relative amount of accumulation of each intermediate, and (iii) the ability to fit the simulations of both the 430 and the 700 nm time courses with the same rate constants.

HPLC Product Analysis. All reactions were carried out under multiple turnover conditions using 5 μM MMOH active sites, 1 μM MMOR, and 5 μM MMOB (50 μM T111Y), 300 μM NADH, and 1.6 mM nitrobenzene in 50 mM MOPS, pH 7.6 to a final volume of 1 mL at 25 °C. The reactions were quenched after 20 min with 3% TFA. The quenched reaction was vortexed for 30 s and centrifuged for 1 min to remove precipitated protein.

The entire reaction volume was injected onto a HPLC system employing an Alltech Econosphere C185 μ 150 × 4.6 mm column. The mobile phase was a linear gradient from 90:10% to 10:90% HPLC grade water/acetonitrile over 15 min at a flow rate of 1 mL/min. Products were detected by monitoring the absorbance at 254 nm and identified based on the known retention times of authentic standards purchased from Sigma. Each peak area was determined by integration using the System Gold HPLC software from Beckman-Coulter, Inc. Because *o*-, *m*-, and *p*-nitrophenol have different extinction coefficients at 254 nm, the integrated peak area was corrected for this value. The percent product formed reported in Table 4 reflects the total amount of each regioisomer divided by the total amount of product.

RESULTS

MMOB Mutants. The four residues of the Quad mutant are located on a loop in the well-ordered central region of the MMOB structure. To elucidate which residues are responsible for the dramatic effects on sMMO kinetics observed for the Quad mutant, two subclasses of the quad mutant were prepared, N107A/S110A (DBL1) and S109A/T111A (DBL2). The two mutants are structurally distinct because the side chains of N107 and S110 are directed toward the core of MMOB, whereas those of S109 and T111 are oriented toward bulk solution, as can be seen in Figure 1. A sequence alignment shows that both N107 and S110 have homologues in several non-heme monooxygenase effector proteins including those from other sMMO systems, toluene monooxygenases, and phenol hydroxylase (*33*). In contrast, S109 and T111 are strictly conserved only in the sMMO systems.

Structural Integrity. The NMR spectra of these mutants and the single mutants described below are similar to that of the structurally characterized WT-MMOB, suggesting that

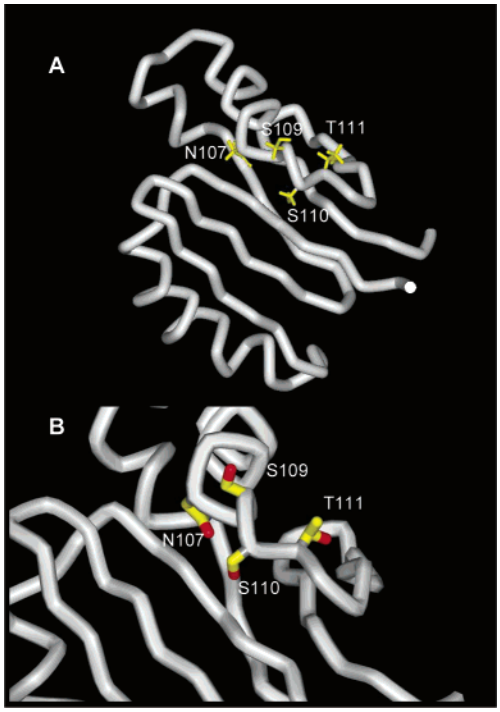

FIGURE 1: Backbone representation of (A) MMOB and (B) the Quad mutant region of MMOB derived from the NMR structure of MMOB from *M. trichosporium* OB3b (*31*). The side chains of the four residues of the Quad mutant are shown in stick representation. The residues with the side-chains pointing out toward solution are Ser109 and Thr111. The residues with the side-chains oriented toward the protein core are Asn107 and Ser110. Each residue was mutated to alanine. MMOB variant DBL1 contained the mutations N107A and S110A, whereas variant DBL2 contained the mutations S109A and T111A.

major structural changes do not occur as a result of the mutation. More significantly, it is shown below that these mutants bind to MMOH with high affinity and promote formation of the intermediates of the MMOH single-turnover cycle, suggesting that the highly specific interactions with MMOH are still fundamentally intact.

Kinetic Analysis of DBL1. The steady-state turnover numbers determined for the reconstituted sMMO system with DBL1 are listed in Table 2.[2] The turnover numbers using nitrobenzene, furan, or methane as the substrate were found to be 2−3-fold lower than when WT-MMOB was used in the assay. These results show that DBL1 elicits a different kinetic response than we reported for the Quad mutant (*33*). In that case, a 2-fold increase in the turnover number was found when large substrates such as nitrobenzene and furan were oxidized, while no change was noted in the maximal rate of methane turnover. As shown in Table 2, use of DBL1 in place of WT-MMOB also resulted in a 3-fold increase in the rate of NADH consumption in the absence of substrates for the reconstituted sMMO system.

The results of single-turnover experiments with DBL1 are presented in Table 3. By monitoring the reaction at the wavelengths where intermediates **P** and **Q** exhibit their maximal absorbances, it was found that **P** was not observed, and **Q** built up to only a minor extent when DBL1 was used

[2] The K_m and V_{max} values for the steady-state turnover of nitrobenzene were determined for each of the MMOB mutants. The K_m was similar for each form of MMOB, and the V_{max} values agreed well with the turnover numbers reported in Table 2.

Table 2: Steady-State Turnover Numbers[2] for the MMOB Mutants[a]

MMOB	none[a]	1.6 mM furan[b]	1.6 mM nitrobenzene[c]	300 μM methane[b]
none	0.081 ± 0.002	0.081 ± 0.003	0.25 ± 0.002[d]	0.079 ± 0.001
WT	0.13 ± 0.01	1.13 ± 0.05	0.3 ± 0.01	1.05 ± 0.01
Quad[e]	0.045 ± 0.01	1.90 ± 0.05	0.50 ± 0.01[f]	1.05 ± 0.01
DBL1	0.37 ± 0.01	0.56 ± 0.02	0.1 ± 0.01	0.52 ± 0.01
DBL2	0.11 ± 0.002	1.40 ± 0.10	0.50 ± 0.01	1.11 ± 0.01
S109A	0.11 ± 0.002	1.11 ± 0.01	0.35 ± 0.01	0.89 ± 0.01
T111A	0.09 ± 0.001	0.79 ± 0.03	0.38 ± 0.01	0.79 ± 0.01
T111Y	0.082 ± 0.002	0.150 ± 0.002	0.04 ± 0.001	0.120 ± 0.001

[a] All experiments were performed at 25 °C and pH 7.6 and are reported in units of s^{-1}. All MMO components (active sites) were present at 1 μM. The turnover number reported is the average of at least four different experiments, and the error is the standard deviation. [b] The turnover numbers were calculated as described in the Experimental Procedures by monitoring NADH consumption at 340 nm. [c] The turnover numbers were calculated as described in the Experimental Procedures by monitoring *p*-nitrophenol formation at 404 nm. [d] Turnover of nitrobenzene in the absence of MMOB was monitored at 340 nm (comparable to values for turnover in the absence of substrate or in the presence of methane or furan) and at 404 nm. No increase in absorption at 404 nm was observed, in contrast to the results observed in the presence of any form of MMOB. The rate reported is for the reaction monitored at 340 nm. [e] Data from ref *33*. [f] Data from current study. Slightly higher turnover numbers than previously reported were observed using either wild type and Quad mutant MMOB.

in place of WT-MMOB, as shown in Figure 2A (compare, for example, with Figure 11). This unexpected observation prevented us from directly studying the effects of substrates on the rate of **Q** decay in detail.

One possible explanation for the near lack of observable intermediates stems from our previous observation that complex formation between MMOH and MMOB is required to make the initial reaction between diferrous MMOH and O_2 nonrate limiting (*10*). It is possible to determine whether complex formation occurs in a catalytically relevant way when DBL1 is used by finding the MMOB/MMOH ratio that maximizes the turnover number. As shown in Figure 3, DBL1 causes the turnover number to maximize at approximately a 1:1 ratio under the conditions used; this is the same as we reported for WT-MMOB (*5*, *25*). This suggests that DBL1 and WT-MMOB each bind to MMOH with high affinities during turnover. Accordingly, in a steady-state competition experiment in which DBL1 and WT-MMOB were present in equimolar amounts, the turnover rate of nitrobenzene turnover was 0.16 ± 0.01 s^{-1}, or roughly the average of the turnover rates observed when the individual MMOBs were used.

A second functional approach to verify MMOB−MMOH complex formation during catalysis is to determine the total yield of *p*-nitrophenol from nitrobenzene oxidation in a single-turnover experiment. The formation of a stoichiometric MMOB−MMOH complex in this reaction causes the yield to double in comparison to that from single-turnover reactions without MMOB or with a modified form of MMOB that cannot form a complex with MMOH (*10*, *32*). As shown in Figure 2B, the maximum optical change because of product formation is different when DBL1 is used in place of WT-MMOB. The lower yield of *p*-nitrophenol in the former case would be consistent with a lack of complex formation. However, we have shown previously that both *p*- and *m*-nitrophenol are formed during the sMMO catalyzed nitrobenzene oxidation (*30*), and the product ratio changes dramatically when MMOB is present. Because the extinction coefficients for *m*- and *p*-nitrophenol at 404 nm are quite different (0.25 and 15 mM^{-1} cm^{-1}, respectively, at pH 7.6), the yield judged from the optical time course can be deceiving. As shown in Table 4, the product distribution determined by HPLC analysis is significantly shifted toward *m*-nitrophenol product formation when DBL1 is used but remains quite different than that observed in the absence of MMOB. When the observed time course is corrected for the relative amounts of the two nitrophenols present, the overall yield is at least 90% of that observed for WT-MMOB, suggesting that a functional complex is formed. Furthermore, the observed shift in regiospecificity of product oxidation suggests that complex formation changes the MMOH active site structure such that substrates approach the reactive oxygen species in a different manner.

Although WT-MMOB and DBL1 exhibit different time courses for formation of *p*-nitrophenol under the single-turnover conditions, as seen in Figure 2B, both time courses can be fit to summed exponential expressions to reveal the *p*-nitrophenol product formation and release rate constants (*33*). This analysis shows that the rate constant for the release of *p*-nitrophenol (**T** decay) with DBL1 is 3-fold less than with WT-MMOB (Table 3). The formation rate constant for *p*-nitrophenol is decreased about 10-fold relative to the case in which WT-MMOB is used. However, it remains faster than that for product release. This *p*-nitrophenol formation rate constant has been shown to be equal to the decay rate constant for **Q** in previous studies (*11*) suggesting that the reaction between **Q** and nitrobenzene is slow when DBL1 is used. This could either arise from an inherently slow reaction, or more likely, because of a slow step in the **Q** formation process that limits the concentration of **Q**. Nevertheless, the formation of the correct products suggests that intermediate **Q** forms, albeit in low maximal concentration.

One approach to determining why intermediates **P** and **Q** are difficult to observe in the single-turnover cycle using DBL1 is to study the rate of oxidation of the diiron cluster. This process is accompanied by a small increase in absorbance at 430 nm that is independent of the intense 430 nm absorbance of **Q**. In the past, we have demonstrated this change by adding a large excess of substrate to the single-turnover reaction (*15*). In this case, **Q** decays very rapidly such that none is observed to accumulate; thus, the **P** formation reaction is unmasked. In the presence of WT-MMOB the increase in extinction coefficient arising from oxidation of the reduced diiron cluster occurs during the formation of the (hydro)peroxy intermediate **P** and normally occurs with a rate constant of about 26 s^{-1} at 4 °C or at least 250 s^{-1} at 25 °C. As shown in Figure 2A when DBL1 was used, the oxidation of the reduced diiron cluster dominates the absorbance change, and the small amount of **Q** that accumulates at the maximum is observed as an overshoot in the time course before a slight decrease in absorbance to the final value as **Q** decays. Fitting the time course to a two exponential process gives an excellent representation of the data and yields rate constants of 13.6 and 0.71 s^{-1}. The rate constant of 0.71 s^{-1} must be assigned to the slow step in the overall process that includes formation of **P***, **P**, and **Q** because if it were assigned to the decay of **Q**, a very significant amount of **Q** would accumulate. The

Table 3: Rate Constants for Reactions Using MMOB Mutants in Transient Kinetic Studies[a]

experimental conditions	kinetic step	rate constants (s^{-1})						
		WT	Quad	DBL1	DBL2	S109A	T111A	T111Y
25 °C pH 7								
no substrate	$\mathbf{P}^{Formation}$	>200		2.16 ± 0.34	>200	>200	>200	3.43 ± 0.29
	$\mathbf{Q}^{Formation}$	57.6 ± 2.03		*60*	65.2 ± 3.16	68.0 ± 2.47	84.4 ± 1.00	*60*
	$\mathbf{Q}^{Decay}$	0.14 ± 0.01		13.5 ± 0.78	0.15 ± 0.01	0.15 ± 0.01	0.15 ± 0.01	0.31 ± 0.02
1 mM furan	$\mathbf{Q}^{Decay}$	41 ± 3.0			106 ± 19	46 ± 8.0	88 ± 12	
0.2 mM furan	$\mathbf{Q}^{Decay}$	6.0 ± 0.1			8.2 ± 0.3	5.5 ± 0.2	9.1 ± 0.3	*≥15*
0.2 mM methane	$\mathbf{Q}^{Decay}$	6.3 ± 0.2			6.4 ± 0.1	5.3 ± 0.2	5.6 ± 0.2	1.6 ± 0.07
25 °C pH 7.6								
no substrate	$\mathbf{P}^{Formation}$	>100		0.71 ± 0.04	>100	>100	>100	1.60 ± 0.22
	$\mathbf{Q}^{Formation}$	31.1 ± 0.5		*40*	45.9 ± 0.9	34.6 ± 0.7	48.9 ± 1.3	*40*
	$\mathbf{Q}^{Decay}$	0.21 ± 0.02		13.6 ± 0.3	0.23 ± 0.01	0.21 ± 0.01	0.21 ± 0.01	0.25 ± 0.01
1.6 mM nitrobenzene	$\mathbf{Q}^{Decay}$	*7*	*45*[b]	*0.75*[c]	*30*	*6*	*40*	*25*
	$\mathbf{T}^{Decay}$	*0.75*	*1.9*[b]	*0.25*	*2.3*	*0.7*	*2.3*	*0.44*
4 °C pH 7								
no substrate	$\mathbf{P}^{Formation}$	10.2 ± 1.6	9.64 ± 1.0[d]	*0.07*	8.6 ± 0.7		12.8 ± 0.31	0.10 ± 0.005
	$\mathbf{Q}^{Formation}$	2.4 ± 0.1	2.45± 0.3[d]	*2.5*	2.6 ± 0.1	2.5 ± 0.1	2.9 ± 0.2	*2.5*
	$\mathbf{Q}^{Decay}$	0.044 ± 0.001	0.045 ± 0.005[d]	*1.0*	0.058 ± 0.002	0.05 ± 0.001	0.047 ± 0.002	0.03 ± 0.001
0.2 mM methane	$\mathbf{Q}^{Decay}$	2.4 ± 0.1			2.1 ± 0.1	2.1 ± 0.04	1.9 ± 0.04	
0.2 mM ethane	$\mathbf{Q}^{Decay}$	3.8 ± 0.2			5.6 ± 0.1			

[a] Each rate constant is the average of at least four different experiments and were determined by nonlinear regression fitting procedures as described elsewhere (*11, 33*) and in the Experimental Procedures. The error reported is the standard deviation in the data. The values for rate constants that are listed in italics were determined by previously published procedures (*15*) employing a combination of nonlinear regression fitting and simulation of the observed time courses (see Experimental Procedures). [b] Values under the current conditions found to be slightly higher than previously reported (*33*). [c] This rate constant probably arises from a step before **Q** formation in the cycle. [d] From ref *33*. **Q** decay in the absence of substrate also exhibited a second phase with a rate constant of 0.12 ± 0.001 s^{-1}.

pH dependence of the reaction (Table 3) suggests that the slow step is, in fact, **P** formation, as described in more detail below. This analysis of the **Q** formation and decay time course suggests that the **Q** decay rate constant is 13.6 s^{-1}, which is a 50-fold increase over the constant observed using WT-MMOB.

Another possibility for the low build-up of **Q** is that **P** decay becomes uncoupled from **Q** formation. However, this is unlikely because the product yield from nitrobenzene turnover is about 90%, so at least this fraction of **P** must be converted to **Q**. A slow step with a rate constant of 0.71 s^{-1} prior to **Q** formation would account for the observed formation rate constant of *p*-nitrophenol in the presence of DBL1 (0.75 s^{-1}) because the rate constants of the steps prior to **Q** decay are independent of substrate concentration (*11*, *15*, *17*). Moreover, the great acceleration of the spontaneous decay rate of **Q** in the presence of DBL1 in combination with the now rate-limiting **P** formation would account for the observed increase in the NADH oxidation rate in the absence of substrates noted in the data shown in Table 2.

Kinetic Analysis of DBL2. The steady-state parameters determined for the reconstituted sMMO system with DBL2 are listed in Table 2. The turnover number using furan or nitrobenzene as the substrate is increased by 1.2- or 1.7-fold, respectively, relative to the case in which WT-MMOB is present. These results are consistent with the rate enhancements previously observed using the Quad mutant. As can be seen in Table 2, no change was observed in the turnover number for methane oxidation using DBL2, again in agreement with the effects of the Quad mutant. In contrast to the results obtained in the presence of DBL1, the rate of NADH consumption by the reconstituted sMMO system was not changed when DBL2 was used in place of WT-MMOB.

The rate constants extracted from single-turnover data when DBL2 was used are presented in Table 3. In the presence of substrate, DBL2 altered the rate of **Q** decay in a manner similar to that which we previously described for the Quad mutant. Relative to the reactions in the presence of WT-MMOB, larger substrates than methane, such as furan or ethane, react with **Q** with an increased rate constant, and large products such as *p*-nitrophenol are released more rapidly as shown in Figure 4. In the case of methane, the rate of **Q** decay was inhibited slightly when DBL2 was used, although not to the same extent as with the Quad mutant. As shown in Figure 5, the amount of **Q** formed in single-turnover reactions in the presence of DBL2 without added substrate is the same as when WT-MMOB was used. Also, both the formation and the decay rate constants for **Q** are unchanged as observed previously for the Quad mutant (see Table 3).

Kinetic Analysis of the Single Mutants of DBL2. To determine whether a single residue was responsible for the catalytic effects observed in the presence of DBL2 and the Quad mutant, the single mutants S109A and T111A were made. The steady-state turnover numbers for the reconstituted sMMO system using each mutant are listed in Table 2. These mutants each elicited nearly the same turnover number for the sMMO catalyzed reaction with nitrobenzene as the substrate. This turnover number is only slightly larger than that observed for the reaction using WT-MMOB. When furan was the substrate, the turnover number using S109A was very similar to that of the reaction using WT-MMOB, but that using T111A was 30% less. The rate of NADH consumption by the reconstituted sMMO system in the absence of substrate and in the presence of either single mutant was approximately the same as when WT-MMOB was used. The turnover number for methane oxidation is decreased slightly when either S109A or T111A is used. Figure 3 shows that, as with DBL1 and DBL2, maximum activity was achieved at a 1:1 ratio of MMOB/MMOH active

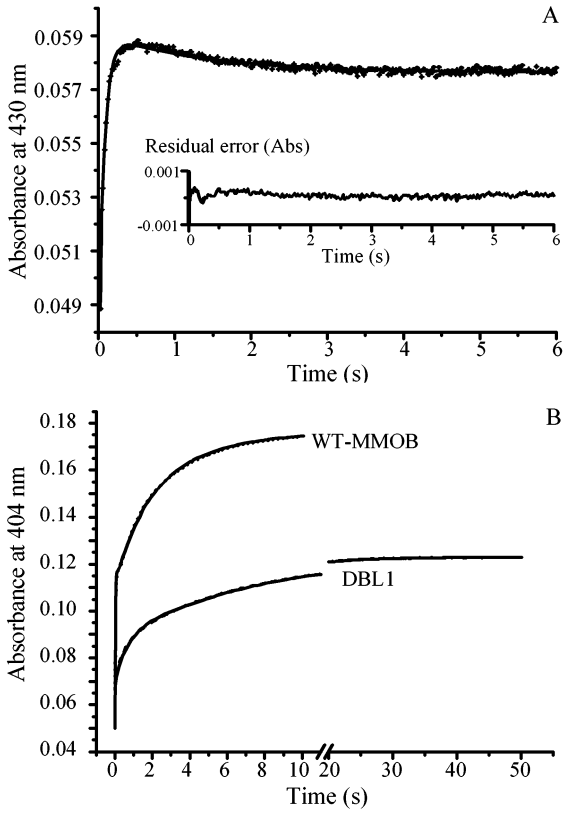

FIGURE 2: Single-turnover reactions with DBL1. In panel A, a single turnover of MMOH in the presence of DBL1 (closed circles) was monitored at 430 nm at 25 °C and pH 7.6 with no substrate added. The data represent the average of three different experiments. The nonlinear regression fit to a two-exponential process is shown as the solid line. The parameters obtained from the fitting procedure were amplitude 1 = 0.013, k_1 = 13.6 and amplitude 2 = −0.0014, k_2 = 0.70. The residual error is plotted on the same scale as the data. In panel B, single turnover of diferrous MMOH using nitrobenzene as a substrate was performed in the presence of DBL1. The reactions with WT-MMOB (dotted line) and DBL1 (dashed line) occurred at 25 °C and pH 7.6. Each time course shown represents the average of at least three different experiments. The concentration of reactants following mixing in the stopped-flow was 42 μM MMOB, 42 μM MMOH (active sites), and 1.6 mM nitrobenzene. The simulation for both WT-MMOB and DBL1 (solid line) is shown superimposed on each data set.

sites for each of the single residue MMOB mutants, demonstrating that they have the same optimal binding ratio as WT-MMOB for MMOH when the enzyme is turning over.

The time course of **Q** formation using either S109A or T111A in the absence of substrate is the same as when WT-MMOB is used (data not shown). However, dramatic changes are observed in the **Q** decay reaction in the presence of substrates using T111A. Figure 6 shows the single-turnover time course of *p*-nitrophenol formation and release using S109A, T111A, and WT-MMOB. The data for S109A and WT-MMOB are nearly superimposable, showing that the rate constants of all the reactions from **Q** formation forward are unchanged, whereas the time course using T111A resembles that of DBL2 (see Figure 4). Accordingly, the rate constant for product release using T111A was found to be 2.3 s^{-1} at 25 °C, which is the same as the rate constant of *p*-nitrophenol release in the presence of DBL2. The rate constant for **Q** decay with furan as the substrate is enhanced 2-fold when T111A is used, and this also agrees well with the 2.5-fold increase observed above using DBL2. The effects on the **Q**

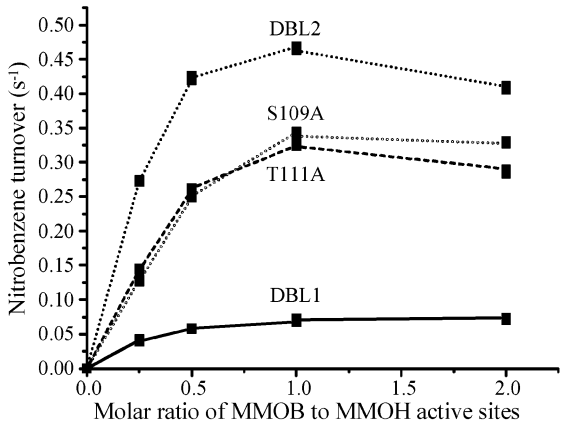

FIGURE 3: Titrations of steady-state nitrobenzene turnover by sMMO with the MMOB mutants. All reaction solutions were at 25 °C, pH 7.6 as described in the Experimental Procedures. The concentration of each MMOB mutant was varied from 0 to 2 μM. The experiment was repeated at least three times at each concentration of MMOB. The entire data set is shown. The lines do not represent a fit of any kinetic model to the data set.

Table 4: Product Distribution from Nitrobenzene Oxidation by the Reconstituted sMMO System with MMOBs

	Percent of Product Formed	
MMOB	*p*-nitrophenol	*m*-nitrophenol
none[a]	10	90
WT	89 ± 1.0	11 ± 1.0
DBL1	69 ± 0.6	31 ± 0.6
DBL2	89 ± 0.6	11 ± 0.6
T111Y	84 ± 2.5	16 ± 2.5

[a] See ref *30*.

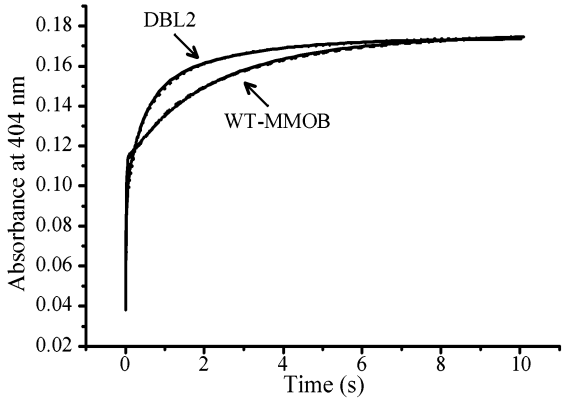

FIGURE 4: Time course of a single-turnover reaction with 1.6 mM nitrobenzene with DBL2 (dotted line) and WT-MMOB (dashed line). Each time course shown is the average of four different experiments. The experimental conditions were identical to those described in the legend of Figure 2B.

time course with 1 mM furan when DBL2, T111A, or WT-MMOB are used are shown in Figure 7. Clearly, the rate of **Q** decay is significantly accelerated in the presence of T111A, although not as much as when DBL2 was used, as shown by the decrease in the amount of **Q** that is accumulated at t_{max} as well as the decrease in the t_{max} value.

The increase of both the rate constant of **Q** decay with furan as the substrate and the rate constant of release of *p*-nitrophenol using nitrobenzene as the substrate in reactions with T111A present strongly suggests that T111 is the key residue to the functions perturbed by the Quad mutant. In

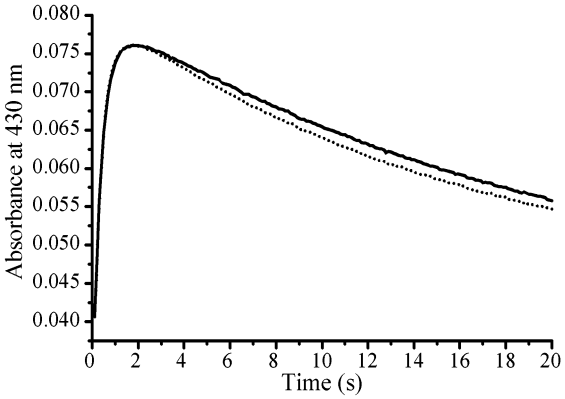

FIGURE 5: Time course for a single-turnover reaction followed at 430 nm with WT-MMOB (solid line) and DBL2 (dotted line). Each reaction was performed at 4 °C and pH 7. The concentration of protein was 23 μM MMOH active sites and 23 μM of each MMOB isoform. The data shown represents the average of four separate experiments.

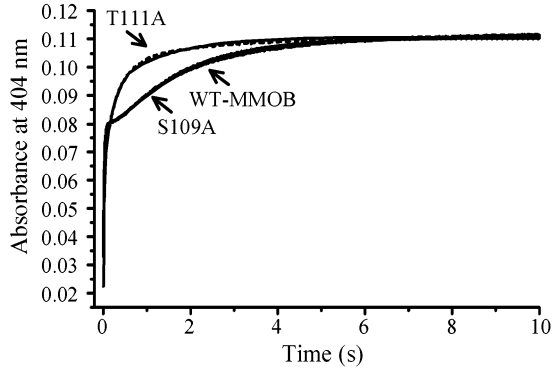

FIGURE 6: Time course of a single-turnover reaction with 1.6 mM nitrobenzene. The data shown are for WT-MMOB (solid line), S109A (open dotted line), and T111A (dashed line). Each time course shown is the average of four different experiments. The data for WT-MMOB and S109A is nearly superimposable. All experiments were performed at 25 °C and pH 7.6 with 23 μM MMOH active sites and 23 μM MMOB. The simulation (solid line) overlays each data set.

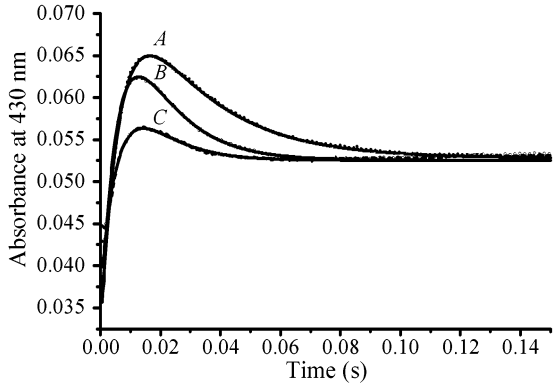

FIGURE 7: Effects of 1 mM furan on the time course at 430 nm at 25 °C, pH 7.6. The time courses shown using WT-MMOB (A), T111A (B), and DBL2 (C) are the average of at least four different experiments. The data for S109A were similar to those for WT-MMOB and are omitted for clarity. The concentration of MMOB and MMOH (active sites) was 23 μM. The results of nonlinear regression fitting procedures are overlaid on each data set.

contrast, S109A causes only minor changes in the rate constants observed for both steady-state and transient kinetic studies relative to those observed for WT-MMOB.

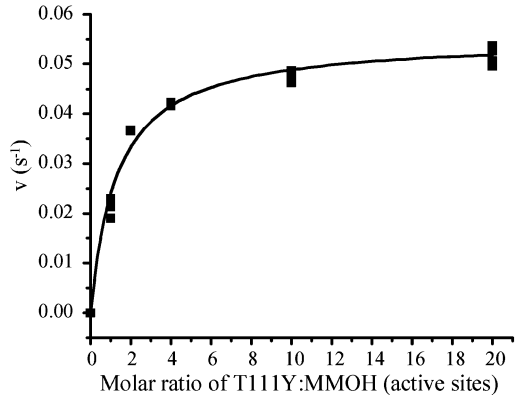

FIGURE 8: Titration of steady-state nitrobenzene turnover with T111Y. The T111Y concentration was varied from 0 to 20 μM. All steady-state assays were performed at 25 °C and pH 7.6 as described in the Experimental Procedures.

Kinetic Analysis of T111Y. In the simplest interpretation of the molecular sieve hypothesis described in the introductory paragraphs, the Quad mutant increases access to the active site by placing smaller residues at a critical component interface. If the bulk of the residue is primarily responsible for the observed effects, then substituting a larger residue that is still sufficiently hydrophilic to be placed on the protein surface, such as tyrosine, might serve to decrease the reaction rates of large substrates.

One concern raised by the mutation of Thr111 to a more bulky residue is that the affinity between MMOB and MMOH might be altered. Figure 8 shows the rate of nitrobenzene oxidation as a function of the relative T111Y concentration. In contrast to WT-MMOB and the mutants discussed thus far, when T111Y was used, the reaction was observed to saturate at a binding ratio of 10:1 relative to MMOH and MMOR. This indicates that the affinity is decreased by this mutation, at least during turnover. Nevertheless, the fact that the reaction rate saturates at high concentrations of T111Y suggests that a complex is being formed. Because of the apparent ~10-fold decrease in affinity between MMOH and T111Y during turnover, all subsequent steady-state and transient kinetic assays were done at a ratio of 10:1 T111Y to MMOH (active sites). Increasing the amount of MMOR present in these reactions did not affect the observed rates.

The effects of T111Y on the sMMO single-turnover reaction are as dramatic as in the steady-state. As can be seen in Figure 9A, in the absence of substrates, very little **Q** is formed when T111Y is used (compare with the time course using WT-MMOB shown in the inset). The reason for this is a large decrease in the rate constant of the rate-limiting step in the **Q** formation process, from 57.6 s^{-1} with WT-MMOB to 3.4 s^{-1} at 25 °C and pH 7. The rate constant of **Q** decay is slightly larger when T111Y is used, 0.31 versus 0.14 s^{-1} with WT-MMOB. Because it has been previously shown that the diferric-(hydro)peroxo intermediate, **P**, directly precedes **Q** (*11*, *14*), the decreased rate constant for **Q** formation suggests that a significant amount of **P** would build-up when using T111Y if the **Q** formation step itself is slow. However, as can be seen in Figure 9A, this is clearly not the case. The absorbance change at 700 nm is quite small, and more instructively, the t_{max} occurs at nearly the same

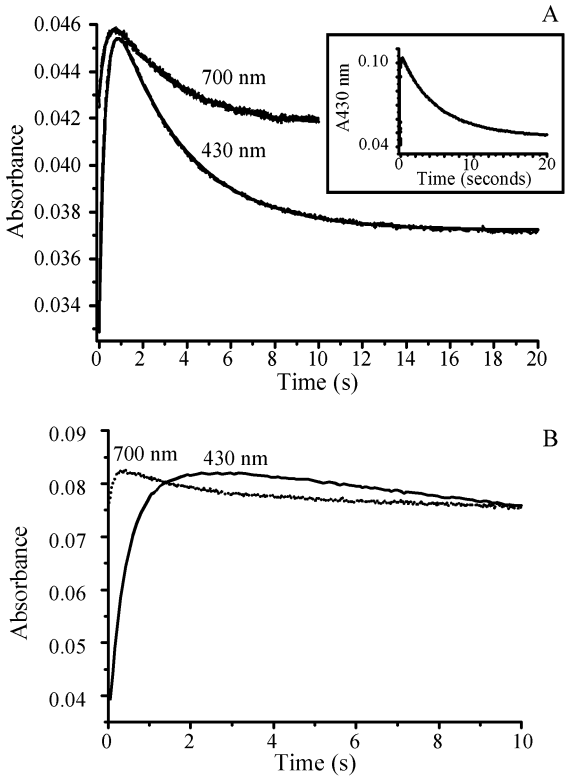

FIGURE 9: Time courses at 430 and 700 nm with T111Y at 25 °C and pH 7 (panel A) and with WT-MMOB at 4 °C and pH 7 (panel B). The 700 nm data is offset by 0.02 absorbance units to allow a comparison. The inset in panel A shows the time course of Q formation and decay with WT-MMOB at 25 °C and pH 7 with 23 μM MMOH active sites and 23 μM MMOB. Following mixing in the stopped-flow, the concentrations of MMOH (active sites) and WT-MMOB were 23 μM for the experiments in panel B, whereas the concentration of T111Y was 230 μM for the experiments in panel A. The data at 430 and 700 nm in the presence of T111Y were subject to nonlinear regression fitting procedures. The fit is superimposed on the data.

time as the species at 430 nm, suggesting that the formation rate constant for **P** has been altered. It has previously been shown that **Q** has a broad UV/vis absorbance spectrum that has a weak but measurable intensity at 700 nm (*11*, *15*, *37*); therefore, the similarity in the t_{max} at each wavelength raises the possibility that the majority of the absorbance at 700 nm in this case may, in fact, be due to **Q**. Using the same reaction conditions, but with WT-MMOB in place of T111Y, intermediate **P** is formed within the dead-time (1.46 ms) of the stopped-flow instrument and is therefore not observed. However, to illustrate the dramatic difference caused by the use of T111Y, Figure 9B shows the time course for **P** and **Q** using WT-MMOB at 4 °C and pH 7. If **Q** formation is not the step that is rate limiting for the reaction using T111Y, then it must be one of the steps leading to the formation of **P**.

The reaction time courses at 340 and 700 nm were simulated using numerical integration techniques as described in the Experimental Procedures. The previously determined rate constants for the steps in the **Q** formation time course using WT-MMOB were replaced one at a time by the experimentally determined value of 3.4 s^{-1} for T111Y. As expected, a simulation in which the **P** to **Q** transformation step was slow did not match experimental results shown in Figure 9A. However, substitution of the 3.4 s^{-1} rate constant

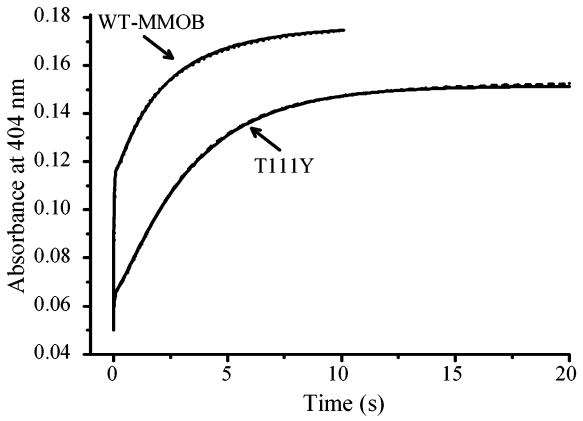

FIGURE 10: Time course at 404 nm from a single-turnover of 1.6 mM nitrobenzene with WT-MMOB (dotted line) and T111Y (dashed line). The concentration of MMOH was 42 μM active sites. The concentration of WT-MMOB was 42 μM, and the concentration of T111Y was 420 μM because of the decreased binding affinity of T111Y for MMOH during turnover. The reaction was performed at 25 °C and pH 7.6. The traces shown represent the average of three different experiments. As described in the text, the simulation of the time course is superimposed on the data.

for any of the steps up to and including **P** formation resulted in a satisfactory simulation at both wavelengths.

A different approach to determine which reaction step is rate limiting is to monitor the pH dependence of the rate constants. We have previously shown that the rate constant for **P** formation decreases substantially as the pH increases (*14*). In the case of T111Y, the rate constant for the positive going phase monitored at 430 nm decreased from 3.4 to 1.6 s^{-1} as the pH was increased from 7.0 to 7.6, while the rate of the negative going phase was unchanged (data not shown). Because only **P** and **Q** formation reactions are pH sensitive, and **Q** formation was concluded not to be the rate-limiting step based on the arguments presented above, the data are most consistent with **P** formation being the rate-limiting step. The same conclusion can be reached from the pH dependence of the slow step in the **Q** formation sequence when DBL1 is used, justifying the conclusion drawn above that the formation of **P** is rate limiting in that case as well.

The time course of nitrobenzene turnover using T111Y and WT-MMOB is shown in Figure 10. The difference at short times is due primarily to the absorbance from **Q**, which is less in the case of the reaction using T111Y. At the completion of the reaction, about 75% as much change in OD from *p*-nitrophenol formation is observed using T111Y in place of WT-MMOB. Product analysis revealed that in the presence of T111Y, the product distribution was slightly shifted, as shown in Table 4. Thus, the decreased ϵ_{404} of *m*-nitrophenol accounts for about half of the difference in absorbance change observed in the presence of T111Y as compared to WT-MMOB. The remainder of the difference in product formed may be the result of uncoupling at some point in the catalytic cycle when this substrate is used. By fitting the entire time course shown in Figure 10, it was found that the rate constant of *p*-nitrophenol release is 0.44 s^{-1} when T111Y is present (Table 3), which is 1.7-fold slower than when using WT-MMOB and nearly 5-fold slower than observed using T111A and DBL2. The rate of **Q** decay was determined to be 5.7-fold faster than when using WT-MMOB.

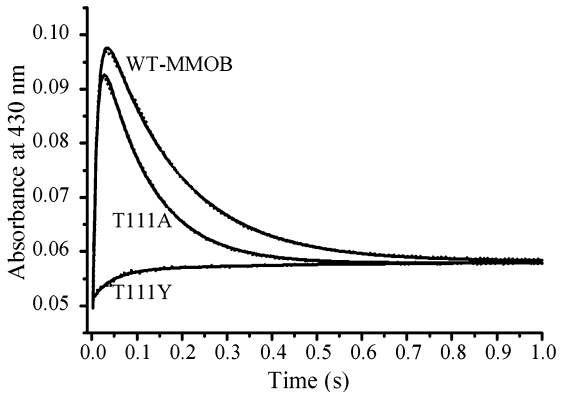

FIGURE 11: Effects of 100 μM furan on the **Q** time course at 25 °C and pH 7 with WT-MMOB, T111A, and T111Y. The time courses shown are the average of four different experiments, and the data are shown as a dotted line. The protein concentrations after mixing in the stopped-flow were 30 μM MMOH active sites and 30 μM WT-MMOB. The concentration of T111Y used was 300 μM because of a 10-fold decreased affinity during turnover for MMOH. The nonlinear regression fit (solid line) to the data is superimposed on the time courses for the cases in which WT-MMOB and T111A were used. The simulation (solid line) to the data is superimposed on the time course in the presence of T111Y.

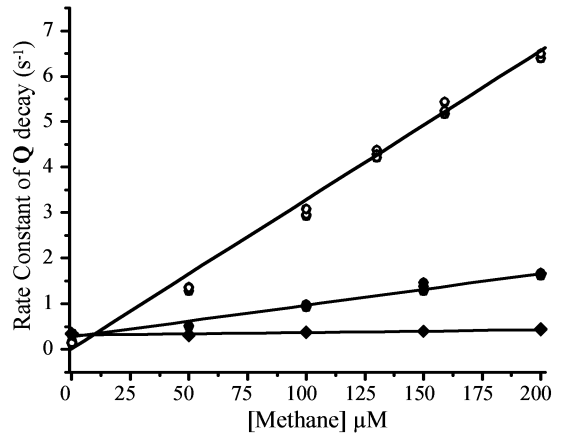

FIGURE 12: Effect of methane on the rate of **Q** decay with T111Y and WT-MMOB. The concentration of methane was varied from 0 to 200 μM in the presence of WT-MMOB (open circles) and T111Y (closed circles). The concentration of d_4-methane was varied from 0 to 200 mM (closed diamonds) using T111Y. The reactions were performed in triplicate, and the entire data set is shown. All reactions were performed under single-turnover conditions with 23 μM MMOH and 230 μM T111Y at 25 °C, pH 7. The data were fit using linear regression to obtain the second-order rate constant. The fit is represented as the solid black line.

The time course of **Q** formation and decay in the presence of 100 μM furan is shown in Figure 11 for single-turnover reactions using T111Y, T111A, and WT-MMOB. Unexpectedly, no **Q** was observed to accumulate in the presence of T111Y. Nonlinear regression fitting of each time course revealed that the rate of **Q** decay for WT-MMOB and T111A was 6.0 ± 0.1 and 9.1 ± 0.3 s^{-1}, respectively. To achieve a good fit to the time course in the presence of T111Y using the simulation procedures described above (see Experimental Procedures), the rate of **Q** decay had to be fixed to a value of at least 15 s^{-1}, so the true value may be significantly greater. Similar results were obtained when the substrates ethane, propane, and butane were used (data not shown). In contrast, as shown in Figure 12, the second-order rate constant for the rate of **Q** decay with methane is 6.9 mM^{-1} s^{-1} at 25 °C when T111Y is used, which is 5-fold slower than when WT-MMOB is used.

It is possible that the failure to observe **Q** in the presence of substrates derives from a reaction of intermediate **P** or one of the other **Q** precursors directly with substrates. This is unlikely in the current case because saturated alkanes are among the substrates that cause this effect, and there is no indication that any intermediate other than **Q** can react with these molecules. To show definitively that **Q** can react with these molecules when T111Y is used, a double mix stopped flow experiment was performed in which diferrous MMOH was first mixed with T111Y and O_2 to form **Q**. After a delay sufficient to allow the **Q** concentration to maximize, substrates were added in a second rapid mix. The reaction rate constants for 100 μM ethane and 100 μM furan were much greater than when WT-MMOB was used; estimates for the **Q** decay rate constants are 380 and 110 s^{-1}, respectively.

A hallmark of the MMOH single-turnover reaction using WT-MMOB is the large ^{2}H KIE of ~50 observed for methane turnover. In the case of T111Y, the KIE is observed to decrease to ~10. The second-order rate constant of **Q** decay for CD_4 oxidation is the same when either WT-MMOB or T111Y is used (0.65 mM^{-1} s^{-1}, 25 °C, pH 7). Thus, the entire change in the KIE can be attributed to a decrease in the rate constant with CH_4 as the substrate. In the case of ethane, no KIE for the **Q** decay reaction is observed when using WT-MMOB, but a value of ~3.5 is observed when using T111Y (k = ~3800 mM^{-1} s^{-1} or ~1100 mM^{-1} s^{-1}, for C_2H_6 or C_2D_6, respectively). The rate constant for reaction of C_2D_2 with **Q** is ~9 times greater than observed using WT-MMOB.

DISCUSSION

It is evident from both our current and past studies that the interaction between the regulatory protein MMOB and the hydroxylase enzyme MMOH profoundly affects the dynamics of the interconversion of intermediates at several steps in the catalytic cycle of the latter (*10*, *33*). Moreover, it appears that structural changes are induced in the active site of MMOH as a result of complex formation with MMOB that alter both the regiospecificity, and at some level, the chemistry of the oxygen insertion chemistry (*30*, *34*). Each of these effects of MMOB is important to the physiological function of sMMO because they combine to allow methane to be oxidized at a much higher rate than would be expected based on its high C−H bond stability. The specific mechanism by which MMOB can affect sMMO chemistry has broad implications for the mechanisms of the many other oxygenase enzymes that utilize effector proteins as well as the role of protein−protein interactions in regulating complex biological systems. These aspects of this study are discussed here.

Potential Mechanisms for Mutant MMOB Effects. Our initial study of the reactions of the Quad mutant of MMOB led to the hypothesis that the amino acid residues in the region of the mutations regulate entry of substrates into the active site of MMOH. The simplest implementation of this hypothesis would be the generation of a channel into the active site as a result of complex formation with the residues in the Quad mutation region forming the mouth of the channel. Changes in properties such as size and hydropho-

bicity of these residues might then be expected to affect the rate of entry of substrates that themselves vary in these same properties. In this model, structural changes would be localized to the residue that was mutated. However, more complex models such as changes in local structure of the MMOB−MMOH interface or changes in the flexibility of the MMOH structure as a result of mutation might also result in easier passage of larger molecules into the MMOH active site. As discussed below, within the group of mutants studied here there is evidence for both the simple and the complex models for the gating effects of MMOB. However, all of the mutants support the underlying hypothesis that MMOB controls the entry of molecules into the active site. It was the goal of this study to begin to examine the effects of the individual mutations within the Quad mutation region on each step of the catalytic process including substrate and product exchange.

Effects of DBL1. The MMOH single-turnover reaction using the DBL1 mutant exhibits distinctly different kinetic behavior and regiospecificity than systems in which either WT-MMOB or any of the other mutants examined here are used. This supports the initial hypothesis that the amino acid residues that extend into the MMOB core structure will have a different effect on the reaction than those that point toward the likely MMOH interface. The steady-state and transient kinetic results obtained when DBL1 was used suggest that neither N107 nor S110 is the residue primarily responsible for causing the rate constant increases observed with the Quad mutant. Thus, they are not the gating residues that regulate substrate entry into the hypothetical MMOH molecular sieve. Nevertheless, the kinetic and modeling studies indicate that these residues do cause major decreases in the rate constants of the **P*** to **P** transformation, as well as an increase in the **Q** decay rate constant and a decrease in the rate constant of **T** decay, showing that they do perturb the reaction in some fundamental ways. Although some of these effects are reminiscent of those observed in the absence of MMOB−MMOH complex formation, this is apparently not the case because the ratio of DBL1 to MMOH needed to maximize the rate of steady-state turnover is the same as that observed for WT-MMOB. The fact that the regiospecificity of hydroxylation of nitrobenzene is different than observed for the reaction both with and without WT-MMOB present suggests that this mutation alters the structure of the MMOH active site so that the substrate is oriented in a unique position. Thus, the DBL1 mutation may fall into the more complex class of mutations discussed above in which broader structural changes on both sides of the MMOB/MMOH interface alter catalysis. As discussed above, WT-MMOB has been shown to alter the structure and/or the electronic environment near the diiron center and to greatly increase at least two rate constants in the oxygen activation process (*25*). Thus, it is reasonable to assume that a different set of changes in the environment of the diiron center might be caused by a mutation of MMOB. Such structural changes may account for the effects on both the **P*** to **P** transformation step and the spontaneous **Q** decay reaction, neither of which require the entry of a substrate into the active site. These steps might be expected to be independent of the gating effect of MMOB, but a conformational change in the active site might well alter the proton donation need for the **P*** to **P** conversion or the inherent stability of **Q**.

Effects of DBL2, S109A, and T111A. In contrast to the DBL1 mutant, three of the mutants involving the residues that extend away from the folded core region of MMOB (DBL2, S109A, and T111A) are all generally similar to WT-MMOB in terms of their effects on the reaction. Most importantly, each of the reaction cycle intermediates can be observed to form in relatively high yield, and the distribution of products from nitrobenzene is essentially unaltered. This suggests that there are no major changes in the stability of the intermediates, and complex formation causes similar changes to the MMOH active site structure as observed using WT-MMOB. The effect of each mutant on sMMO steady-state turnover maximizes at about 1:1 mutant MMOB to MMOH, so each mutant binds strongly to MMOH during catalysis as observed for WT-MMOB. Thus, these mutants may fall into the mutant class described above in which alteration of the residues that gate entry into the MMOH active site changes the access properties into the site without introducing a new set of global conformational changes. The increase in the turnover rate of furan and nitrobenzene in the sMMO catalyzed steady-state reactions, the increase in the rate of *p*-nitrophenol release in a single-turnover of nitrobenzene, and the increased rate of **Q** decay with furan as the substrate in the presence of DBL2 are all in good agreement with the results of the Quad mutant experiments reported previously. This suggests that one or more of the residues altered in DBL2 are primarily responsible for the effects of the Quad mutant. In some manner, these mutations mask or compensate for the effects of the other residues changed in the Quad mutant that were revealed using the DBL1 mutant. Of the two single residue mutants, S109A is very much like WT-MMOB in all of its effects on catalysis, whereas T111A is similar to DBL2 and the Quad mutant. Consequently, Thr111 appears to be the primary residue involved in the proposed gating effects of the Quad mutant.

One difference between T111A and the Quad and DBL1 mutants is that the increase in the steady-state turnover number for nitrobenzene is slightly less than the increase in rate constant for **T** decay. There is also a small decrease in the steady-state turnover numbers for methane and furan, which is not expected based on the molecular sieve hypothesis. Because all of the rate constants in the catalytic single-turnover cycle can be measured and are faster than the turnover numbers, this suggests that a step other than **T** decay has become at least partially rate limiting for T111A. One possibility is that product release actually occurs in two or more steps, and only the first is observable using ionization of *p*-nitrophenol to detect the release process.[3] Another possibility is that a structural reorganization is required after product release to allow the next cycle to begin and that this process is not as fast when T111A is used. A third possibility stems from the fact that, in contrast to the single-turnover system, MMOR is present during steady-state turnover. This component has both electron transfer and effector roles, and it increases the rate of product release in the wild-type reconstituted sMMO system (*25*). It is not currently known how a change in the MMOB structure will influence either

[3] In the analysis of the Quad mutant time course using nitrobenzene as the substrate, a intermediate following **T** (**T1**) was required for an adequate fit (*33*). The optical properties of **T1** were similar to those of *p*-nitrophenol in solution but with a slightly smaller extinction coefficient.

of these MMOR roles. If these roles are altered, effects on the steady-state turnover number might be observed. There is currently no way to distinguish between these possibilities.

Effects of T111Y. It was expected that placing tyrosine at the interface of the MMOB−MMOH complex would slow the binding of large substrates relative to the rates observed with alanine and threonine in this position. According to the molecular sieve model, this change should slow the rate constants of steps in which substrates bind to, or products dissociate from, the enzyme. In support of the original premise, the reaction of methane with **Q** and the product release step, as measured by **T** decay for nitrobenzene turnover, are slower than observed for WT-MMOB. However, there are several observations that suggest T111Y is not acting as expected according to the model. For example, the turnover number determined under steady-state conditions is much less than the rate constant for **T** decay, suggesting that the largest effect of T111Y on turnover may come after product release. Also, the step in which substrate binds, **Q** decay, is much faster for T111Y than for WT-MMOB for all substrates except methane in direct contradiction to the model. Finally, the spontaneous rate of **Q** decay in the absence of substrates is faster using T111Y in place of WT-MMOB, suggesting that the inherent stability of **Q** may have been altered. There are also several observations that suggest the interaction of MMOH with T111Y is different than with WT-MMOB. These include the fact that the affinity of T111Y for MMOH during turnover examined by the ratio required for maximal rate is decreased 10-fold relative to the value for WT-MMOB. Also, the regioselectivity of nitrobenzene oxidation is perturbed, and the slow step in **Q** formation is apparently shifted to the **P*** to **P** transformation. These latter changes are argued above to be indicative of a different conformational change in MMOH than is caused by WT-MMOB. On the basis of these observations, it seems likely that T111Y is a mutant that exhibits both perturbation of the substrate gating effect and more global structure changes. Thus, T111Y could be described as a hybrid of the two classes of mutants discussed above.

The significant increase in the rate constant of the reaction of most substrates with **Q** when T111Y is present might have several origins based on alteration of the interface structure. However, it is intriguing to consider the possibility that the need to accommodate the steric bulk of T111Y in the interface results in an increase in access by forcing a structural change in MMOH in a region removed from the normal substrate access point. One model that contrasts the effects of the two T111 mutants with WT-MMOB is shown in Scheme 2. This scheme has found some experimental support in our ongoing structural studies.[4,5]

Q *Reaction with Methane in the Presence of Mutant MMOBs.* It is interesting to note that for the MMOB mutants, the rate constant for **Q** decay in the presence of methane is in most cases smaller than observed when using WT-MMOB.

Scheme 2: Hypothesis for the Effects of MMOB and MMOB Mutants at Position 111 on Catalysis[a]

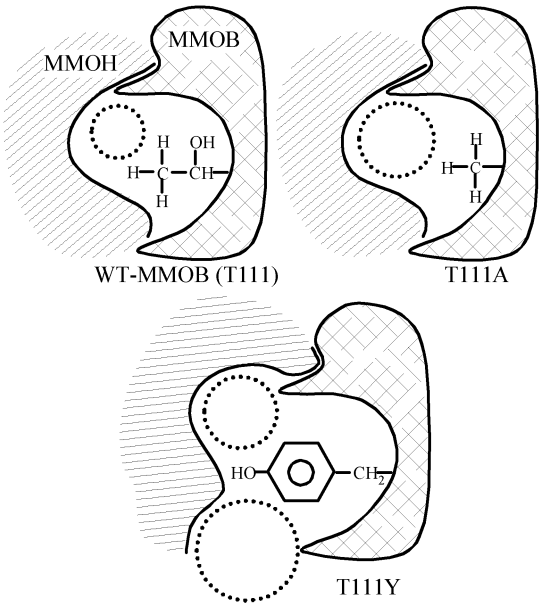

[a] The complex between MMOH and MMOB is proposed to gate substrates into the active site based at least in part on size. Both T111A and T111Y appear to increase access to large substrates but for different reasons as described in the text. The dashed circles represent hypothetical access channels or regions of increased structural flexibility.

In the case of T111Y, the rate constant of **Q** decay with 200 μM methane was nearly 4-fold lower at 25 °C than when WT-MMOB was used. This might be interpreted as the new tyrosine blocking access to the active site except for the fact that the rate constant for CD_4 as the substrate is unchanged. Because larger substrates are observed to react very rapidly with **Q** for this mutant, it seems unlikely that the binding of methane is rate limiting. A selective decrease in the rate constant for **Q** reaction with methane was also observed for the Quad mutant. In that case, it was also observed that the rate constant for CD_4 was unchanged, giving a large decrease in the KIE (50 reduced to 6) and leading to speculation that a large tunneling component of the reaction between the activated oxygen of **Q** and the methane had been lost (*34*). The contribution of quantum mechanical tunneling in other enzyme systems that catalyze H-atom abstraction has been shown to be extremely sensitive to the structure of the active site (*38*−*42*). Consequently, even small changes in structure caused by the MMOB mutants may be sufficient to perturb the specific site in which methane must bind to allow a significant tunneling component. Interestingly, no other substrate shows evidence for a significant tunneling component in their reactions with **Q** with any form of MMOB, so the putative binding site by may be specific for methane

[4] Our recent results suggest that, in the MMOH−MMOB complex, MMOB Thr111 occupies a space between two MMOH helices near the active site. If this is the case, then it is reasonable that a smaller residue such as Ala would allow passage of a larger substrate without extensive conformational changes. In contrast, a larger residue such as Tyr would not fit in the space occupied by the Thr; thus, a larger conformational change in MMOH might occur, leading to less substrate discrimination (Brazeau and Lipscomb, unpublished).

[5] The proposal here that the residues of the Quad mutant are near the interface with MMOH and the active site is not supported by a recent magnetic resonance study using *Methylococcus capsulatus* Bath components, which places the region mutated in the quad mutant away from the MMOH active site (*47*). However, it is worthwhile noting that placing large spin labels (*47*) in MMOB from *M. capsulatus* Bath at the putative site of MMOH−MMOB interaction revealed by the magnetic resonance study was not reported to perturb the interaction between MMOH and MMOB. In contrast, placing large groups at position T111 within the quad mutant region clearly perturbs the MMOH−MMOB interaction as shown here supporting this as one interface site.

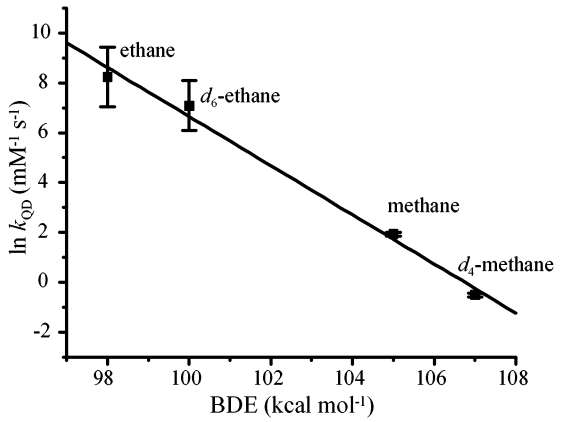

FIGURE 13: Dependence of the rate of **Q** decay on bond strength in the presence of T111Y. The natural log of the approximate second-order rate constant for **Q** decay with ethane, methane, and their deuterated analogues is plotted as a function of the C−H bond dissociation energy (BDE). The data for ethane and d_6-ethane were obtained from double mix stopped-flow experiments as described in the Experimental Procedures. The data for methane and d_4-methane were obtained as in Figure 12. The solid line is a linear fit to the data.

even in the wild-type sMMO system. These results suggest that the mechanism of the reaction between **Q** and methane is different than that for other substrates, at least to the extent that tunneling effects play an important role in catalysis.

Use of T111Y to Evaluate the Relationship of Bond Dissociation Energy to Reaction Rate Constant. It is interesting to note that despite its high bond dissociation energy (BDE), methane has one of the highest turnover numbers in steady-state catalysis and exhibits one of the largest rate constants for reaction with **Q** in the single-turnover system. On the basis of the current and previous studies, we propose that this is due to the combined effects of restricted access, which makes binding rate limiting for large substrates and tunneling effects specifically on the methane reaction. The exceptionally high rate constant for reaction of large substrates with **Q** and the apparent loss of significant tunneling effects for the methane reaction suggests that, when T111Y is used, the effects of both restricted access and tunneling are greatly mitigated. Accordingly, as shown in Figure 13, the BDEs of d_4-methane, methane, d_6-ethane, and ethane now correlate well with the observed rate constants of the reaction with **Q** reported above. This supports mechanistic theories in which the C−H bond of methane is broken specifically in the **Q** decay reaction.

*Oxidase Reaction and Spontaneous **Q** Decay.* Past studies have linked MMOB to changes in the rate of NADH consumption in the absence of substrate (*9*). We would argue based on an assessment of the effects of MMOB on the interconversion of intermediates in the reaction cycle that it affects uncoupled NADH consumption in two ways. First, MMOB gates O_2 into the active site of MMOH to allow electrons from MMOR to enter an oxygen activation cycle rather than being shunted to oxygen directly to yield hydrogen peroxide (*10*). Second, the current work indicates that MMOB affects the stability of **Q** as well as the rate constants leading to its formation. Consequently, higher uncoupled rates of NADH consumption will be observed for a mutant MMOB like DBL1, which decreases the stability of **Q** by accelerating its decay.

The increase in **Q** decay rate constant when DBL1 is present also reveals the complex kinetic relation of steps within the catalytic cycle. For a slow substrate such as nitrobenzene, it is shown in Table 2 that DBL1 actually slows the reaction below the turnover rate observed in the absence of substrate. This may be due to the fact that substrate causes **Q** to convert rapidly to **T,** which decays slowly in the DBL1 case, as indicated in Table 3. Thus, a shift in the rate-limiting step between **P** formation and product release causes the unusual substrate linked deceleration.

Relationship to Small Effector Proteins in Other Enzyme Systems. A sequence alignment of the effector proteins from sMMO systems of four methanotrophs shows that the four residue sequence V108-S109-S110-T111, which overlaps with the residues altered in the Quad mutant, is strictly conserved (*33*). Small effector proteins have also been found for other diiron-containing oxygenase enzymes such as toluene-4-monooxygenase (T4MO) from *Pseudomonas mendocina* (*43*), toluene-3-monooxygenase (T3MO) from *Pseudomonas picketti* (*44*), toluene-2-monooxygenase (T2MO) from *Burkholderia cepacia* G4 (*45*), and phenol hydroxylase from *Pseudomonas sp.* CF600 (*46*). Sequence alignment revealed that the equivalent of position 111 is occupied by leucine in T2MO, phenylalanine in T3MO and T4MO, and isoleucine in phenol hydroxylase. The fact that threonine 111 is conserved only in the methanotrophs suggests that it may play an important role in selecting for methane in accord with the results presented here.

Bearing on the Regulation of sMMO Catalysis. Our original study of the effects of MMOB mutants on catalysis suggested that individual regions in the MMOB structure control the kinetics of specific steps in the MMOH catalytic cycle (*33*). In that work, four mutants were identified that altered five different steps in the cycle. The current work shows that there are at least overlapping effects on the rates of specific cycle steps for different regions of MMOB. More restrictive mutations in the Quad region affect steps in both the O_2 activation segment of the cycle leading to **Q** and the hydrocarbon oxidation segment, which uses up **Q**. Moreover, a probable new step following the last observed intermediate **T** is revealed in this work and shown to be controlled by MMOB in some manner. It now seems better to view MMOB as a protein that uses several regions of its structure to mediate the reaction between the activated binuclear iron cluster of **Q** and the substrate. There appear to be two aspects to this, both of which are strongly influenced by the structure of the active site. The first is access, which is generally enhanced for large substrates by mutations to smaller residues in the region of the Quad mutant and vice versa. The exception to this is T111Y where organic substrate binding monitored by the rate constant for **Q** decay is accelerated, but product release is slowed. Nevertheless, even in this mutant, alteration of MMOB greatly affects small molecule access into the active site of MMOH in accord with the general model that this is a major role for the regulatory protein. The second aspect is a change in the active site structure that affects many elements of the metal cluster environment and the reaction regiospecificity but most importantly appears to establish the conditions for efficient C−H tunneling for methane oxidation. The combination of access and tunneling appear to restore the competitive advantage to methane that is lost because of its high C−H

bond strength. Mutations in the interface region of MMOB are, to varying degrees, less able to establish this special binding site for methane; thus, the competitive advantage of methane is lost.

REFERENCES

1. Wallar, B. J., and Lipscomb, J. D. (1996) *Chem. Rev. 96*, 2625−2657.
2. Feig, A. L., and Lippard, S. J. (1994) *Chem. Rev. 94*, 759−805.
3. Brazeau, B. J., and Lipscomb, J. D. (2000) *Subcell. Biochem. 35*, 233−277.
4. Merkx, M., Kopp, D. A., Sazinsky, M. H., Blazyk, J. L., Muller, J., and Lippard, S. J. (2001) *Angew. Chem., Int. Ed. 40*, 2782−2807.
5. Fox, B. G., Froland, W. A., Dege, J. E., and Lipscomb, J. D. (1989) *J. Biol. Chem. 264*, 10023−10033.
6. Rosenzweig, A. C., Frederick, C. A., Lippard, S. J., and Nordlund, P. (1993) *Nature 366*, 537−543.
7. Elango, N., Radhakrishnan, R., Froland, W. A., Wallar, B. J., Earhart, C. A., Lipscomb, J. D., and Ohlendorf, D. H. (1997) *Protein Sci. 6*, 556−568.
8. Lund, J., and Dalton, H. (1985) *Eur. J. Biochem. 147*, 291−296.
9. Green, J., and Dalton, H. (1985) *J. Biol. Chem. 260*, 15795−15801.
10. Liu, Y., Nesheim, J. C., Lee, S.-K., and Lipscomb, J. D. (1995) *J. Biol. Chem. 270*, 24662−24665.
11. Lee, S.-K., Nesheim, J. C., and Lipscomb, J. D. (1993) *J. Biol. Chem. 268*, 21569−21577.
12. Lee, S.-K., Fox, B. G., Froland, W. A., Lipscomb, J. D., and Münck, E. (1993) *J. Am. Chem. Soc. 115*, 6450−6451.
13. Liu, K. E., Wang, D., Huynh, B. H., Edmondson, D. E., Salifoglou, A., and Lippard, S. J. (1994) *J. Am. Chem. Soc. 116*, 7465−7466.
14. Lee, S.-K., and Lipscomb, J. D. (1999) *Biochemistry 38*, 4423−4432.
15. Brazeau, B. J., and Lipscomb, J. D. (2000) *Biochemistry 39*, 13503−13515.
16. Shu, L., Nesheim, J. C., Kauffmann, K., Münck, E., Lipscomb, J. D., and Que, L., Jr. (1997) *Science 275*, 515−518.
17. Nesheim, J. C., and Lipscomb, J. D. (1996) *Biochemistry 35*, 10240−10247.
18. Deeth, R. J., and Dalton, H. (1998) *J. Biol. Inorg. Chem. 3*, 302−306.
19. Whittington, D. A., Valentine, A. M., and Lippard, S. J. (1998) *J. Biol. Inorg. Chem. 3*, 307−313.
20. Siegbahn, P. E. M., Crabtree, R. H., and Nordlund, P. (1998) *J. Biol. Inorg. Chem. 3*, 314−317.
21. Lipscomb, J. D., and Que, L. (1998) *J. Biol. Inorg. Chem. 3*, 331−336.
22. Shteinman, A. A. (1998) *J. Biol. Inorg. Chem. 3*, 325−330.
23. Brazeau, B. J., Austin, R. N., Tarr, C., Groves, J. T., and Lipscomb, J. D. (2001) *J. Am. Chem. Soc. 123*, 11831−11837.
24. Guallar, V., Gherman, B. F., Miller, W. H., Lippard, S. J., and Friesner, R. A. (2002) *J. Am. Chem. Soc. 124*, 3377−3384.
25. Fox, B. G., Liu, Y., Dege, J. E., and Lipscomb, J. D. (1991) *J. Biol. Chem. 266*, 540−550.
26. Davydov, A., Davydov, R., Graslund, A., Lipscomb, J. D., and Andersson, K. K. (1997) *J. Biol. Chem. 272*, 7022−7026.
27. Pulver, S. C., Froland, W. A., Lipscomb, J. D., and Solomon, E. I. (1997) *J. Am. Chem. Soc. 119*, 387−395.
28. DeRose, V. J., Liu, K. E., Lippard, S. J., and Hoffman, B. M. (1996) *J. Am. Chem. Soc. 118*, 121−134.
29. Davydov, R., Valentine, A. M., Komar-Panicucci, S., Hoffman, B. M., and Lippard, S. J. (1999) *Biochemistry 38*, 4188−4197.
30. Froland, W. A., Andersson, K. K., Lee, S.-K., Liu, Y., and Lipscomb, J. D. (1992) *J. Biol. Chem. 267*, 17588−17597.
31. Chang, S. L., Wallar, B. J., Lipscomb, J. D., and Mayo, K. H. (1999) *Biochemistry 38*, 5799−5812.
32. Chang, S. L., Wallar, B. J., Lipscomb, J. D., and Mayo, K. H. (2001) *Biochemistry 40*, 9539−9551.
33. Wallar, B. J., and Lipscomb, J. D. (2001) *Biochemistry 40*, 2220−2233.
34. Brazeau, B. J., Wallar, B. J., and Lipscomb, J. D. (2001) *J. Am. Chem. Soc. 123*, 10421−10422.
35. Fox, B. G., Froland, W. A., Jollie, D. R., and Lipscomb, J. D. (1990) *Methods Enzymol. 188*, 191−202.
36. Bradford, M. M. (1976) *Anal. Biochem. 72*, 248−254.
37. Valentine, A. M., Stahl, S. S., and Lippard, S. J. (1999) *J. Am. Chem. Soc. 121*, 3876−3887.
38. Kohen, A., and Klinman, J. P. (1998) *Acc. Chem. Res. 31*, 397−404.
39. Kohen, A., Cannio, R., Bartolucci, S., and Klinman, J. P. (1999) *Nature 399*, 496−499.
40. Kohen, A., and Klinman, J. P. (2000) *J. Am. Chem. Soc. 122*, 10738−10739.
41. Tsai, S.-C., and Klinman, J. P. (2001) *Biochemistry 40*, 2303−2311.
42. Kohen, A., and Klinman, J. P. (1999) *Chem. Biol. 6*, 191−197.
43. Whited, G. M., and Gibson, D. T. (1991) *J. Bacteriol. 173*, 3010−3016.
44. Byrne, A. M., Kukor, J. J., and Olsen, R. H. (1995) *Gene 154*, 65−70.
45. Newman, L. M., and Wackett, L. P. (1995) *Biochemistry 34*, 14066−14076.
46. Nordlund, I., Powlowski, J., and Shingler, V. (1990) *J. Bacteriol. 172*, 6826−6833.
47. MacArthur, R., Sazinsky, M. H., Kühne, H. Whittington, D. A., Lippard, S. J., and Brudvig, G. W. (2002) *J. Am. Chem Soc. 124*, 13392−13393.

BI027429I